J Fluoresc (2007) 17:319–329
DOI 10.1007/s10895-007-0175-3

ORIGINAL PAPER

Application of Asymmetric Model in Analysis of Fluorescence Spectra of Biologically Important Molecules

Aleksandar Kalauzi · Dragosav Mutavdžić · Daniela Djikanović · Ksenija Radotić · Milorad Jeremić

Received: 21 December 2006 / Accepted: 22 February 2007 / Published online: 30 March 2007
© Springer Science+Business Media, LLC 2007

Abstract Having a valid mathematical model for structureless emission band shapes is important when deconvoluting fluorescence spectra of complex molecules. We propose a new asymmetric model for emission spectra of five organic molecules containing aromatic ring: catechol, coniferyl alcohol, hydroquinone, phenylalanine and tryptophan. For each molecule, a series of emission spectra, varying in excitation wavelength, were fitted with the new model as well as with two other analytical expressions: log-normal, described previously in the literature, and sigmoid-exponential. Their deconvolution into two, three and four Gaussian components was also performed, in order to estimate the number of symmetric components needed to obtain a better fitting quality than that of the asymmetric models. Four subtypes of the new model, as well as the log-normal one, did not differ significantly in their fitting errors, while the sigmoid-exponential model showed a significantly worse fit. Spectra of two mixtures: hydroquinone–coniferyl alcohol and hydroquinone–tryptophan were deconvoluted into two asymmetric and four Gaussian components. Positions of asymmetric components of mixtures matched those of separate molecules, while Gaussian did not. Component analysis of a polymer molecule, lignin, was also performed. In this more complex case asymmetric and Gaussian components also grouped in alternating positions.

A. Kalauzi · D. Mutavdžić · D. Djikanović · K. Radotić (✉) · M. Jeremić
Center for Multidisciplinary studies of the University of Belgrade, Despota Stefana, 142 Belgrade, Serbia
e-mail: xenia@ibiss.bg.ac.yu

M. Jeremić
Faculty of Physical Chemistry, University of Belgrade, Studentski Trg, 12-16 Belgrade, Serbia

Keywords Mathematical models · Nonlinear fitting · Monofluorophore · Binary mixture · Lignin

Introduction

Fluorescence spectroscopy, as a very sensitive and informative method for characterization of simple and complex molecules, has a wide application in both analytical and diagnostic studies. The analysis of fluorescent spectra of polymeric molecules is especially complex, since they may contain different fluorophores or one fluorophore in various microenvironments. Therefore, it is necessary to use computer methods for numerical deconvolution of complex emission spectra into individual components. In some of these approaches, only the number of constituent components was determined, or additionally their shapes revealed, without a mathematical model that describes them analytically – like the parallel factor analysis [1, 2]. Therefore, it is of crucial importance to use a valid mathematical model of the emission spectrum of a fluorophore. Some of the widely used analytical expressions describing the components, such as Gaussian and Lorentzian, suffer from a basic drawback. They are symmetric, contrary to the majority of experimentally recorded emission spectra. Asymmetry is a consequence of the fact that vibration force constants of the ground and excited states are not the same. To our knowledge, only few attempts to obtain analytical equation of a fluorescence band shape can be found in the literature. Siano and Metzler [3] proposed the log-normal distribution, as an asymmetric model for the absorption spectra of the hydroxypyridine derivatives in solution. Burstein and Emelyanenko [4] used its mirror-symmetric form as a model for emission spectra of different classes of organic fluorophores. Burstein et al. [5] applied this model to deconvolute spectra of proteins

containing tryptophan fluorophore in different microenvironments.

In this study we propose a new model for the emission spectrum of a fluorophore. We have applied the model to five different molecules of great biological interest, all of them containing aromatic ring: catechol, coniferyl alcohol, hydroquinone, phenylalanine and tryptophan, and tested the model on their two binary mixtures. All spectra were fitted with two existing four-parametric models (log-normal and sigmoid-exponential) and their fitting errors compared to four versions of the new model, also containing four parameters. Simultaneously, we performed deconvolution of spectra of these five molecular species into two, three and four Gaussian components. This was done in order to determine the required number of symmetric components for which the deconvolution becomes more precise than that using the asymmetric models. In addition, this parallel fitting enabled us to compare the corresponding positions of maxima of the asymmetric and symmetric (Gaussian) components, as the excitation wavelength changed. This relationship was studied for all five molecular species and their two binary mixtures, as well as for a multifluorophore molecule, poplar lignin, with the aim to test whether asymmetric models have advantages in deconvolution of fluorescence spectra of complex molecules.

Materials and methods

Steady-state fluorescence spectroscopy. Fluorescence spectra were collected using a Fluorolog-3 spectrofluorimeter (Jobin Yvon Horiba, Paris, France) equipped with a 450 W xenon lamp and a photomultiplier tube. The monofluorophore compounds and poplar lignin were dissolved in deionized water and in dioxane/water 9/1 (v/v), respectively, in a 1-cm optical path length quartz cuvette. The slits on the excitation and emission beams were fixed at four and two nanometers respectively. The spectra were corrected for dark counts. In each measurement, three scans with one-second-integration time, were averaged. The emission spectrum of the solvent (water or dioxane/water) was subtracted. All measurements were performed at controlled temperature of 25°C by means of a Peltier element.

For each of the five molecular species studied, their two binary mixtures, as well as the polymer, a series of emission spectra were measured by varying excitation wavelengths with 5 nm steps. In order to include all geometric characteristics of an emission spectrum into modeling, initial excitation wavelength was set in such a way that recording of emission spectra started 30–40 nm before the sharp rise in emission.

Nonlinear fitting of all fluorescence spectra, for all nine models, was performed using the Nelder-Mead simplex algorithm implemented in Matlab 6.5.

The model. Here we propose a new model describing the shape of the emission band, intended primarily for important biological molecules containing substituted benzene ring

$$F_\lambda = \frac{a}{f_1(b,\lambda)} \frac{1}{(\exp(cf_2(d,\lambda)) - 1)},$$

where F_λ stands for fluorescence intensity at wavelength λ; a, b, c and d represent the model parameters, while f_1 and f_2 may be either exponential or power functions of λ. Depending on the choice for f_1 and f_2, four versions of the model can be distinguished: f_1 and f_2 exponential (conveniently marked as **ee**); f_1 exponential, f_2 power (**ep**); f_1 power, f_2 exponential (**pe**); f_1 and f_2 power (**pp**):

$$\mathbf{ee}: F_\lambda = \frac{a}{\exp(b\lambda)} \frac{1}{\exp(c\exp(d\lambda)) - 1}; \tag{1a}$$

$$\mathbf{ep}: F_\lambda = \frac{a}{\exp(b\lambda)} \frac{1}{\exp(c(\lambda^d)) - 1}; \tag{1b}$$

$$\mathbf{pe}: F_\lambda = \frac{a}{\lambda^b} \frac{1}{\exp(c\exp(d\lambda)) - 1}; \tag{1c}$$

$$\mathbf{pp}: F_\lambda = \frac{a}{\lambda^b} \frac{1}{\exp(c(\lambda^d)) - 1}. \tag{1d}$$

Another four-parametric analytical expression, used previously to describe shapes of both absorption and emission spectra of different molecular classes [4], is the log-normal model (**logn**):

$$\begin{cases} F_\lambda = F_m \exp\{-(\ln 2/\ln^2 \rho) \\ \qquad \times \ln^2[(1/a' - 1/\lambda)/(1/a' - 1/\lambda_m)]\}, \quad \text{for } \lambda > a' \\ F_\lambda = 0, \quad \text{for } \lambda \le a' \end{cases}$$

where F_m is the maximal intensity, ρ the spectral shape asymmetry parameter, a'–function limiting point and λ_m–wavelength at which a maximal fluorescence occurs. Since our spectra were obtained as functions of λ, we substituted wavenumbers with wavelengths and original parameter a with its reciprocal value a'. However, in order to match the symbols for parameters with other four-parametric models, the fit was performed with the following expression

$$\begin{cases} F_\lambda = a \exp\{-(\ln 2/\ln^2 b) \\ \qquad \times \ln^2[(1/c - 1/\lambda)/(1/c - 1/d)]\}, \quad \text{for } \lambda > c. \\ F_\lambda = 0, \quad \text{for } \lambda \le c \end{cases}$$

However, not every four-parametric analytical expression, having a similarity in shape with the recorded spectra, is suitable for modeling the monofluorophore fluorescence emission band. To verify this, we also included an independent four-parametric expression: sigmoid-exponential function (abbreviation for this model **sgme**):

$$F_\lambda = Sg(\lambda)Ex(\lambda) = a\frac{1}{1+c\exp(d\lambda)}\exp(b\lambda),$$

F_λ representing again fluorescence intensity at wavelength λ; *a, b, c* and *d,* the model parameters. In this model, a well known sigmoid shape, $Sg(\lambda)$, is modified by multiplying it with an exponential factor $Ex(\lambda)$, forcing it to decay as λ increases.

The fact that all newly proposed expressions contain four parameters allowed us to compare directly their mean square fitting errors (per point):

$$\overline{e2} = \frac{1}{N}\sum_{i=1}^{N}(y_f(i) - y_e(i))^2, \tag{2}$$

where N stands for the number of points in the spectrum, $y_e(i)$ for the emission intensity of the ith spectral point and $y_f(i)$ for value of the fitted curve in the same point.

Finally, we fitted all spectra with a sum of two, three and four Gaussian components (model abbreviations: **g2**, **g3** and **g4**):

$$F_\lambda = \sum_{i=1}^{n}\frac{A_i}{\sqrt{2\pi}\sigma_i}\exp\left(\frac{-(\lambda-\lambda_{0i})^2}{2\sigma_i^2}\right), \quad n = 2, 3, 4.$$

Since each Gaussian component could be described with three parameters (A_i, σ_i and λ_{0i} – area, width and position, respectively), total number of parameters for this model was *3n* (six, nine and twelve), *n* being the number of components. Therefore, it was not possible to compare mean fitting errors of this deconvolution to four-parametric model errors directly. However, we could get an insight into the rate of fitting error reduction as *n* increases, by estimating the number of components at which this error was smaller than the four-parametric model errors ("dimensional saving").

We used *F*-test to check the hypothesis of equality of mean square errors between the following pairs of models (all four-parametric): **ep**-**logn**, **ep**-**sgme** and **logn**-**sgme**, input variances being summed for experimental points of all spectra measured for each molecular species, divided by the total number of points.

For each molecular species, as well as the studied mixtures and polymer, positions of component maxima, obtained for a series of spectra with varying excitation wavelength, were treated as random variables. In order to calculate an approximate distribution of the probability density for positions of all the components, we constructed corresponding histograms of component maxima positions. However, since histogram profiles (positions and relative amplitudes of histogram maxima) depended on the number of histogram abscissa intervals, we calculated the corresponding approximate probability density distribution by weighed averaging of histogram values for a set of histograms, where interval number varied $h_n = 2, \ldots, h_{\mathrm{n\,max}}$, where h_{nmax} defined fineness of the analysis.

Results and discussion

Except in few cases, for each molecular species, an order of models can be noticed, referring to their mean square fitting errors and regardless of the excitation wavelength (Fig. 1). In other words, error curves on each panel of Fig. 1 were positioned in layers, without decussating. This circumstance allowed us to sort the tested models, for each molecular species, based on the series of their averaged fitting error values over the used excitation wavelengths. Besides, errors of models **ee**, **ep**, **pe**, **pp** and **logn** formed a band on every panel of Fig. 1, and were therefore drawn with solid lines, since they had similar values for a particular excitation wavelength. However, of all the four-parametric models, **sgme** showed a significantly higher error, for all five molecules. This result suggests that the number of model parameters itself is not a decisive factor in determining the precision of mathematical description of a fluorophore emission spectrum. In other words, one cannot use any existing four-parametric formula describing an asymmetric "sharp-rise-slow-decay" process as an emission model. Mathematical structure of the analytical expression of a model plays an important role in its ability to describe the underlying physical processes.

Parallel to nonlinear fitting of the emission spectra with the above-mentioned models, we performed deconvolution of the spectra into Gaussian components (**g2**, **g3**, **g4**), although they differ in the number of parameters from all the others (six, nine, twelve, respectively). This was done in order to determine the number of Gaussian components at which the mean square fitting error falls below the errors of models positioned within the band. As can be seen in Fig. 1, for catehol, phenylalanine and tryptophan, this occurred for **g3** and **g4**, while for coniferyl alcohol and hydroquinone only for **g4**. Siano and Metzler [3] stated four reasons why a systematic study of the shape of monofluorophore spectra should be carried out. Accepting their argumentation, we can only add that by using one of the asymmetric four-parametric models, positioned within the described "error band," one acquires a considerable saving in the number of dimensions of parametric space in which nonlinear fitting is

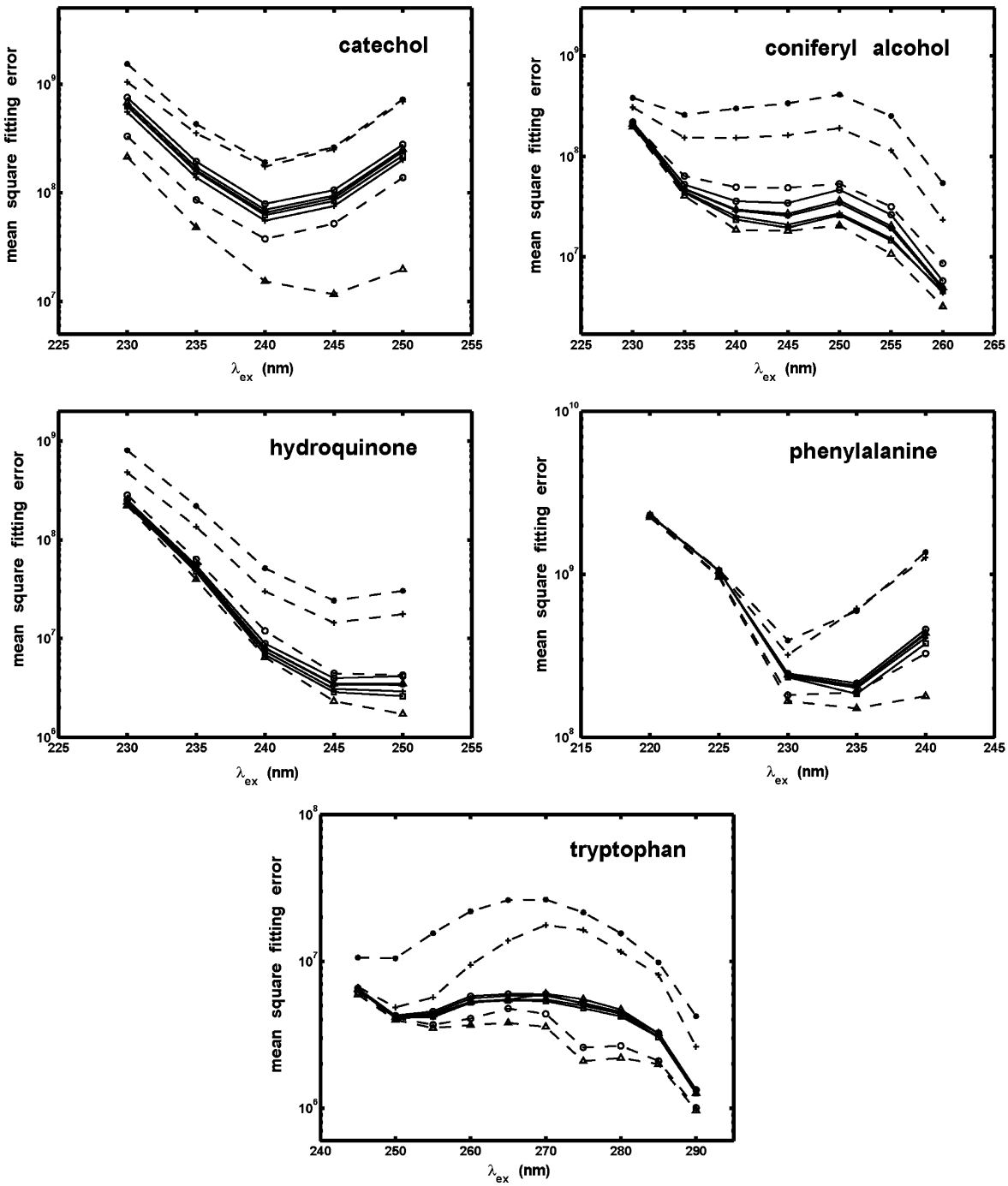

Fig. 1 Mean square fitting errors (per point), calculated according to (2), for nine models, applied to five monofluorophore molecules. For each molecule, a series of spectra was fitted, differing in the excitation wavelength (λ_{ex}). Model marks: (-∗) **ee**; (-+) **ep**; (-o) **pe**; (-Δ) **pp**; (-□) **logn**; (--∗) **sgme**; (--+) **g2**; (--o) **g3**; (--Δ) **g4**

performed. The extent of dimensional saving may be well illustrated by the fact that in cases of catehol, phenylalanine and tryptophan, six-parametric **g2** model was a worse fit than the four-parametric "error band" models (**ee**, **ep**, **pe**, **pp** and **logn**), while for coniferyl alcohol and hydroquinone this extended even to the nine-parametric **g3** model. This further underlines importance of the choice of component analytical expression for deconvoluting complex emission spectra.

Trying to reach a general assessment of a model efficacy in describing emission band shapes for all analyzed molecular species, we had to define some additional averaging of the fitting errors. By modifying formula (2), if $(\lambda_{em})_i$ and $(\lambda_{ex})_j$ denote the *i*th emission and *j*th excitation wavelength,

respectively, expression for the mean square fitting error at excitation wavelength $(\lambda_{ex})_j$ can be written as

$$\overline{e2} = ((\lambda_{ex})_j) = \frac{1}{N}\sum_{i=1}^{N}(y_f((\lambda_{em})_i, (\lambda_{ex})_j) - y_e((\lambda_{em})_i, (\lambda_{ex})_j))^2,$$

while formula for the averaged square fitting error over all excitation wavelengths, for a specific molecular species MS_k, $k = 1, \ldots, 5$ and for a particular model MD_l,$1 = 1, \ldots, 9$, becomes

$$\overline{e2}_{av}(MS_k, MD_l) = \frac{1}{M}\sum_{j=1}^{M}\overline{e2}((\lambda_{ex})_j) = \frac{1}{MN}\sum_{j=1}^{M}\sum_{i=1}^{N}(y_f(\lambda_{em})_i, (\lambda_{ex})_j) - y_e((\lambda_{em})_i, (\lambda_{ex})_j))^2,$$

where M stands for the number of excitation wavelengths. Since fluorescence intensity, and consequently $\overline{e2}_{av}(MS_k, MD_l)$, for a particular molecular species, depend on a number of factors (such as substance concentration, system amplification, etc.), it is not possible to compare intermolecular fitting errors directly. Therefore, we calculated relative values of these errors:

$$\overline{re2}_{av} = (MS_k, MD_l) = \frac{\overline{e2}_{av}(MS_k, MD_l)}{\frac{1}{9}\Sigma_{l=1}^{9}\overline{e2}_{av}(MS_k, MD_l)} \quad (3)$$

These results are presented on Table 1.

Data in Table 1 allow us to arrange the four-parametric models as a series with ascending values of $\overline{re2}_{av}(MS_k, MD_l)$ for each molecular species. According to the last right column, we performed this procedure for all five molecular species, yielding the following order of models concerning their efficacies: **ep**, **logn**, **ee**, **pp**, **pe**, **sgme**. However, although this particular order was established according to the results obtained in this work, one must bear in mind that differences between errors among the "band" models are not significant, as shown in Fig. 2 for **ep** vs. **logn** as an example. Therefore, in case of repeated experiments with these, or some other monofluorophore molecules, we expect that alterations in the presented sequence might occur. However, a significantly greater error of the **sgme** model could be expected again. Of all newly proposed models (**ee**, **ep**, **pe** and **pp**), **ep** was chosen as the most efficient one (Table 1, right column) to be compared with the remaining four-parametric models (**logn** and **sgme**) in terms of error significance. These results are presented in Fig. 2.

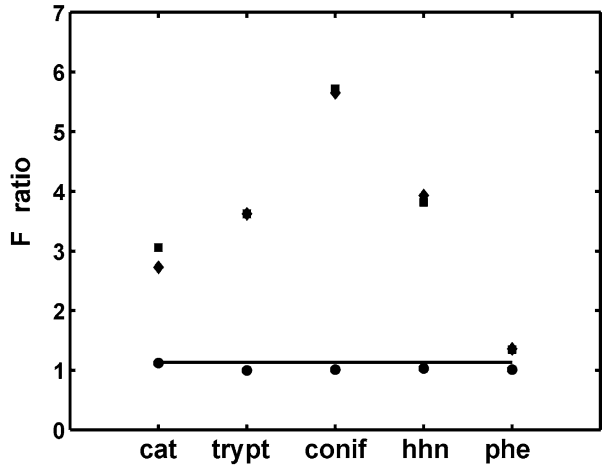

Fig. 2 F-ratio of the mean square errors for some pairs of four-parametric models: (•) **ep** vs. **logn**; (■) **ep** vs. **sgme**; (♦) **logn** vs. **sgme**. Critical F value is 1.132, marked with the horizontal solid line

Mean square error of the **sgme** model was significantly higher in comparison with both **ep** and **logn** models, while there was no statistically significant difference between errors of the **ep** and **logn** models.

At this point it is not clear whether, and to which extent, analytical expression of the newly proposed model reflects actual physical processes during the fluorescence emission.

Table 1 Relative mean square fitting errors, averaged over excitation wavelengths, calculated according to (3) for five molecular species and nine tested models

Model	Np#	Catechol	Tryptophane	Coniferyl alc.	Hydroquinone	Phenylalanine	Mean*
ee	4	0.8472	0.7560	0.5752	0.6944	0.9479	0.7641
ep	4	0.7291	0.7224	0.5328	0.6699	0.9427	0.7194
pe	4	1.0044	0.7650	0.6610	0.7355	0.9574	0.8246
pp	4	0.8972	0.7517	0.5909	0.6982	0.9494	0.7775
logn	4	0.8163	0.7153	0.5389	0.6501	0.9337	0.7309
sgme	4	2.2371	2.6292	3.1420	2.5640	1.2914	2.3727
g2	6	1.7907	1.5700	1.7388	1.5362	1.2588	1.5789
g3	9	0.4587	0.5764	0.7357	0.8331	0.8879	0.6984
g4	12	0.2193	0.5140	0.4847	0.6187	0.8307	0.5335

*Errors from the five columns averaged over five molecular species.

#Number of parameters

Related to this, it is not possible yet to establish any physical meaning of the parameters involved in the model. However, since expressions (1a–1d) may be observed as a generalization of the sum of a geometrical progression, one cannot exclude that in future a deeper link could be established between these expressions or their modifications and a sum of emission terms connected with the transitions to different vibration levels.

Distributions of probability densities of component positions, obtained by parallel deconvolution into two-component Gaussian (**g2**) and two one-component asymmetric models (**logn** and **ep**), for all five molecular species, are presented in Fig. 3.

As can be seen, fitting with both asymmetric models (**logn** and **ep**) resulted in nearly identical, very sharp probability densities of component positions. Numerical values of

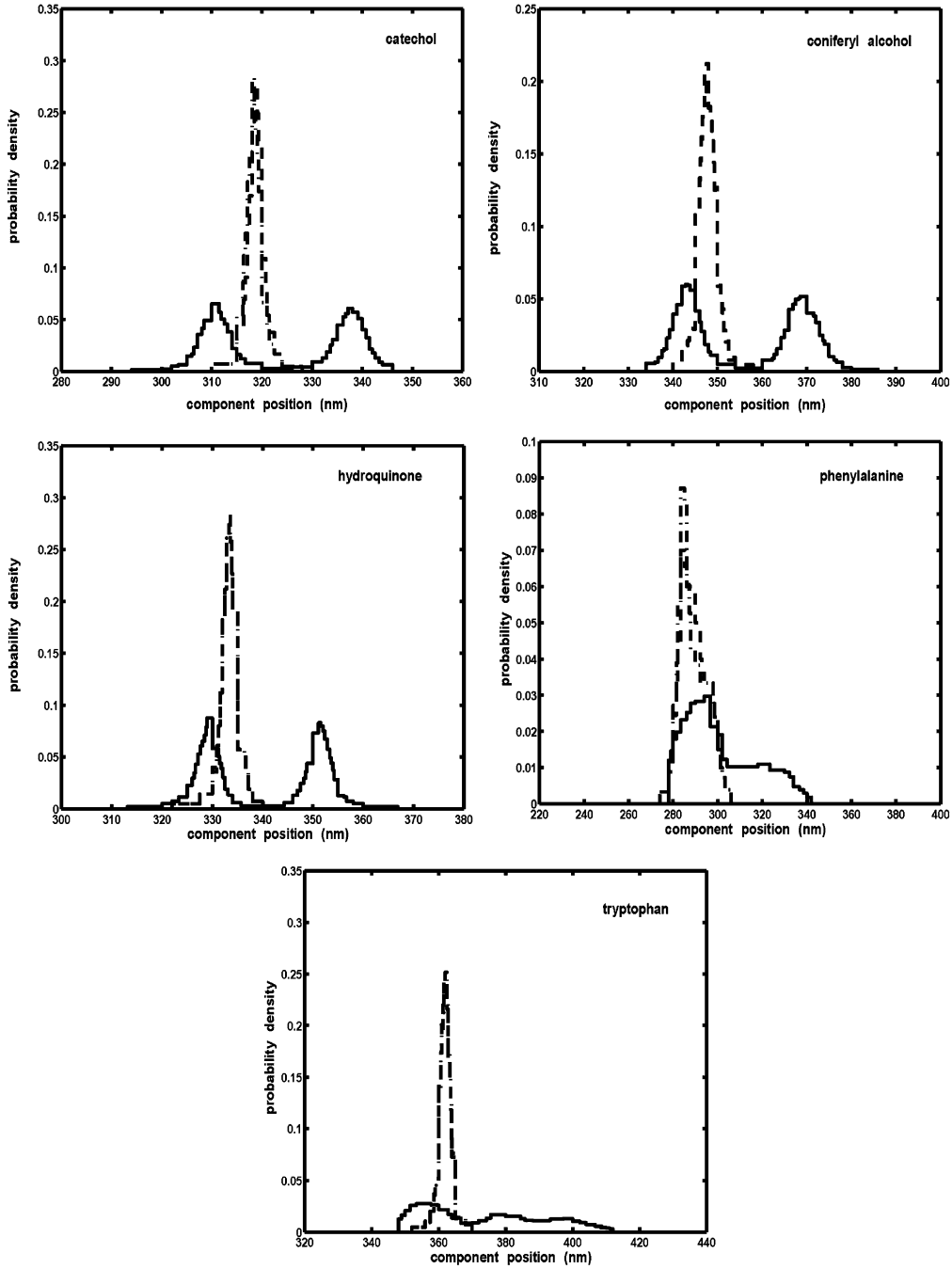

Fig. 3 Approximate distributions of probability densities of component positions for the five analyzed molecular species. Line marks: (- - -) **logn**, (-.-) **ep**, (—) **g2**. Fineness of the analysis: $n_{h\,max} = 20$. Distributions for both asymmetric models (**logn** and **ep**) are almost identical and sharp, allowing a precise determination of the emission maximum for each molecule. Usually, Gaussian components are significantly shifted

Table 2 Maxima of the probability density distributions, presented in Fig. 3, obtained by fitting of emission spectra of the five analyzed monofluorophore molecular species, with two asymmetric models

Model	Catechol	Tryptophane	Coniferyl alc.	Hydroquinone	Phenylalanine
ep	318.2	362.2	347.3	333.5	283.8
logn	318.9	362.0	347.8	333.5	283.9

probability density maxima positions for asymmetric models are presented in Table 2.

Deconvolution into two Gaussian components showed a significant shift of their probability density maxima from the values obtained by fitting with the asymmetric models. The only exception was phenylalanine. Since its emission band shape is close to symmetric, one of the two Gaussian components showed a tendency to position itself in the same

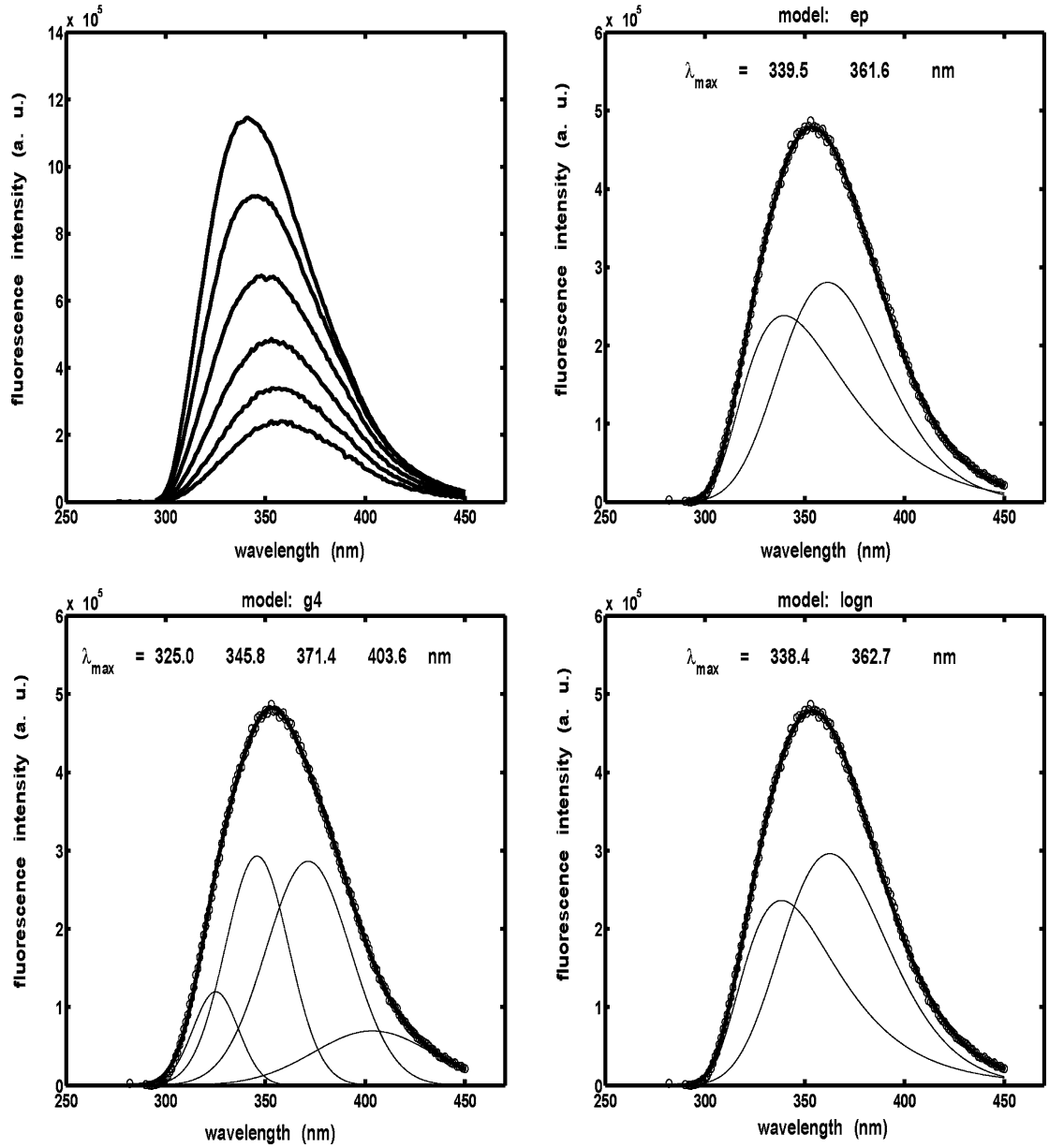

Fig. 4 Upper left panel: Emission spectra of the binary mixture of tryptophan and hydroquinone for excitation wavelengths in the range 250–275 nm with 5 nm step, higher emission intensities corresponding to greater excitation wavelengths. Upper right panel: Result of deconvolution of the emission spectrum obtained by excitation at 260 nm into two components defined by the **ep** model. Circles, measured spectra; solid lines, separate components (thin) and their sum (thick) fitted to the experimental data. Fitted component maxima (λ_{max}) are noted above the curves. Analogous explanation is valid for the two lower panels, presenting deconvolution using **logn** (right) and **g4** (left) models

region as the asymmetric ones. Even so, the corresponding Gaussian probability density peak was much less sharp than any of the two asymmetric peaks. Determining the location of the probability density distribution peak, in case of asymmetric models, may be comprehended as a new method for measuring the wavelength of emission maximum of one-fluorophore molecule. This approach is based on narrow and sharp profiles of all the probability distributions obtained. Moreover, it could be regarded as more precise than conventional techniques used, which were usually performed by detecting the maximum of one emission spectrum.

According to data presented in Fig. 3, two mixtures were chosen to test the distributions of asymmetric vs. symmetric component positions. The first mixture contained coniferyl alcohol and hydroquinone, as their emission maxima are mutually very close. The second consisted of tryptophan and hydroquinone, having more distant emission maxima. Since a monofluorophore molecule contains one fluorophore,

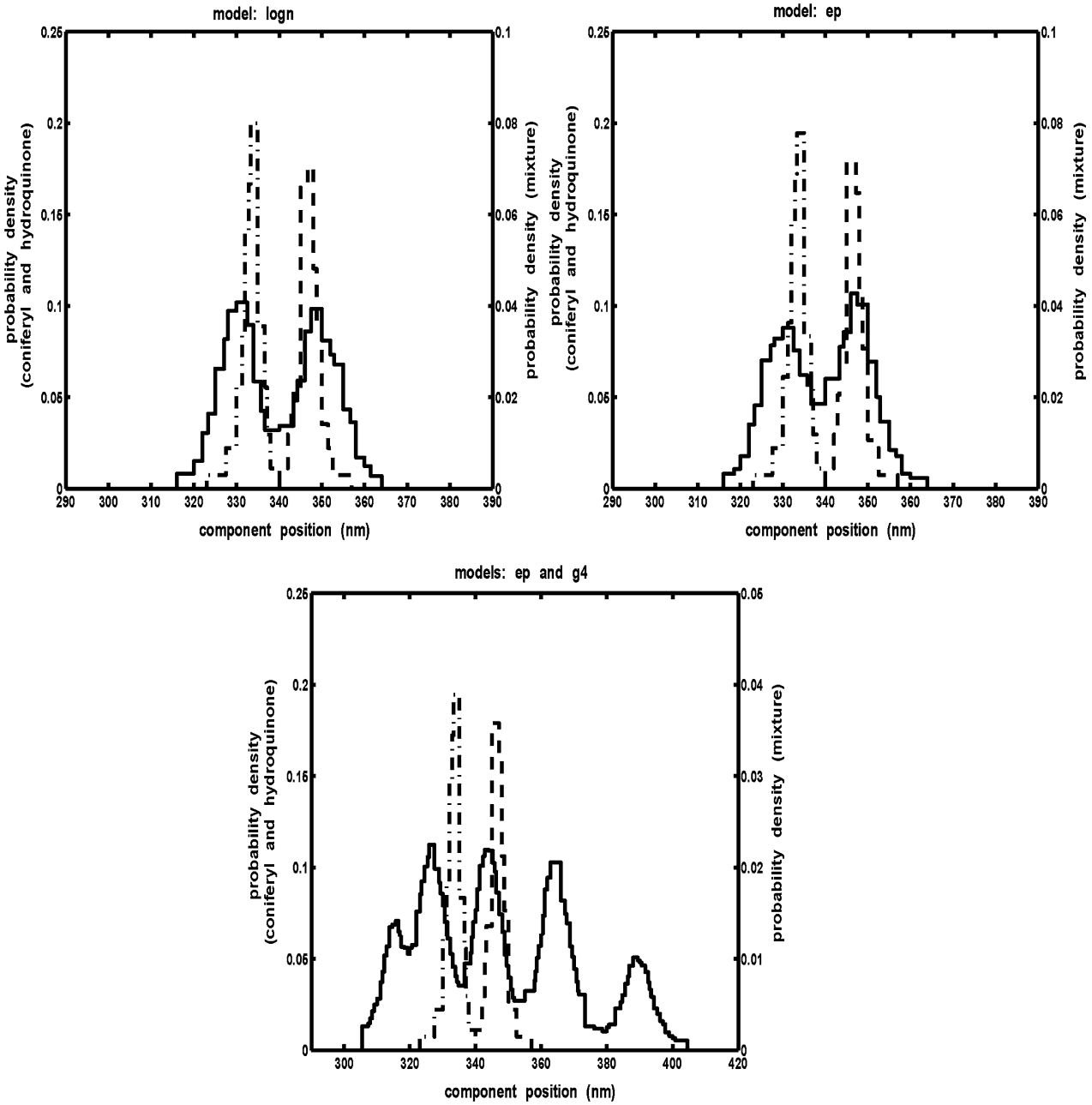

Fig. 5 Approximate distributions of probability densities of component positions for the binary mixture of coniferyl alcohol and hydroquinone (molar concentration ratio 4:1), as well as for the two corresponding separate molecules. Line marks: (- - -) coniferyl alcohol, (-.-) hydroquinone, (—) mixture. Fineness of the analysis: $n_{h\,max} = 10$. Distributions of asymmetric component positions in case of mixture match those for the separate molecules, while Gaussian do not

position of its emission maximum does not depend on the excitation wavelength. However, spectra of a multifluorophore system, such as a mixture of two molecular species, vary in a more complex manner when the excitation wavelength is changing. Emission spectra, recorded from the mixture of molecules with close positions of their separate emission bands, are usually characterized by only one maximum, the position being dependent on the excitation wavelength (visible in case of both tested mixtures). This phenomenon is a consequence of the fact that the two fluorophores are not evenly excited at different wavelengths. The mixture of tryptophan and hydroquinone, as an example, is presented in Fig. 4, upper left panel. Without a numerical method for spectral deconvolution, it would not be possible to identify the corresponding component positions. Although all six spectra of this mixture were deconvoluted into two **ep,** two **logn** and four Gaussian components, only the spectrum excited at 260 nm is presented as an example

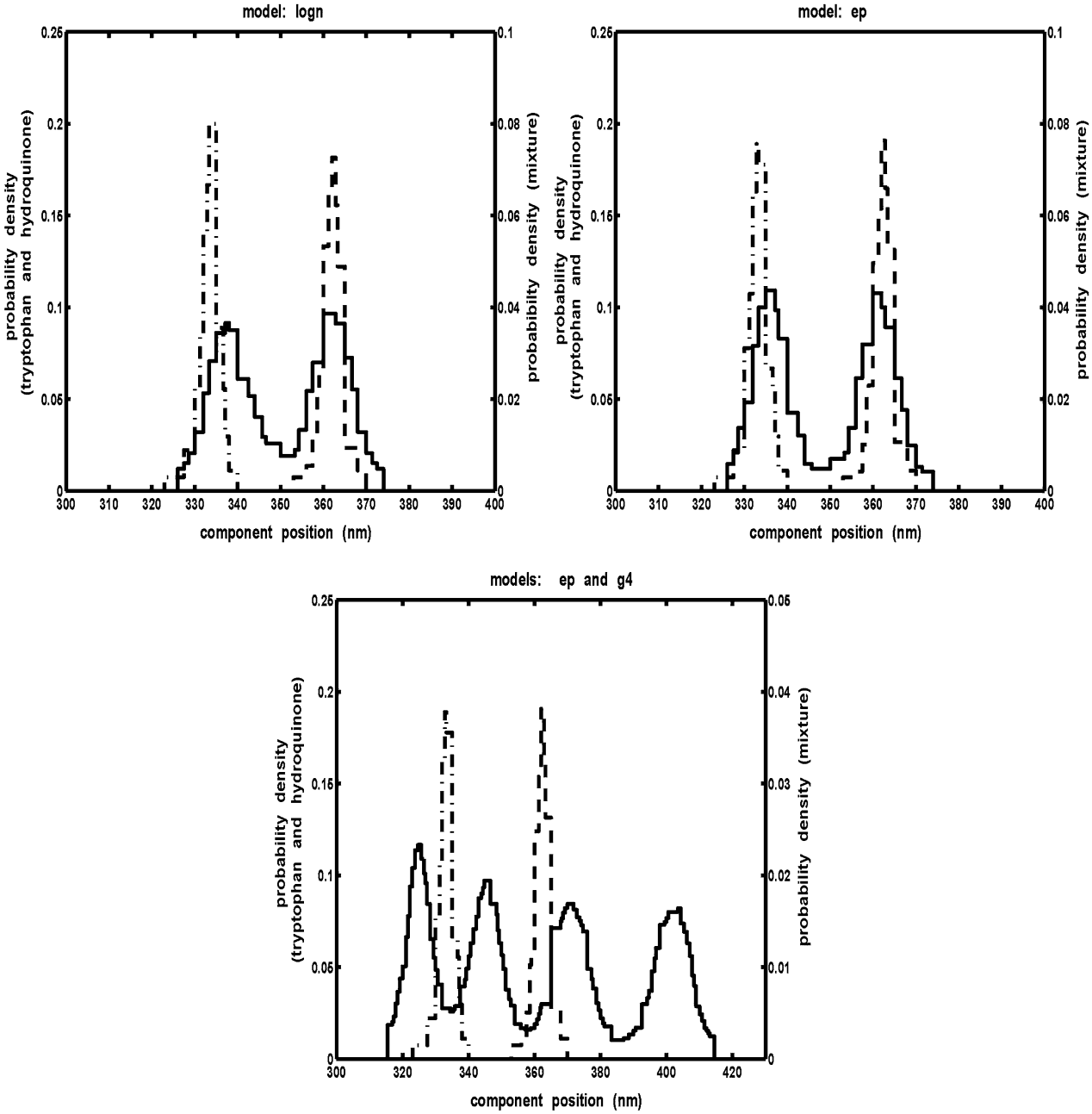

Fig. 6 Approximate distributions of probability densities of component positions for the binary mixture of tryptophan and hydroquinone (molar concentration ratio 1:6) and for the two corresponding separate molecules. Line marks: (- - -) tryptophan, (-.-) hydroquinone, (—) mixture. Fineness of the analysis: $n_{h\,max} = 10$

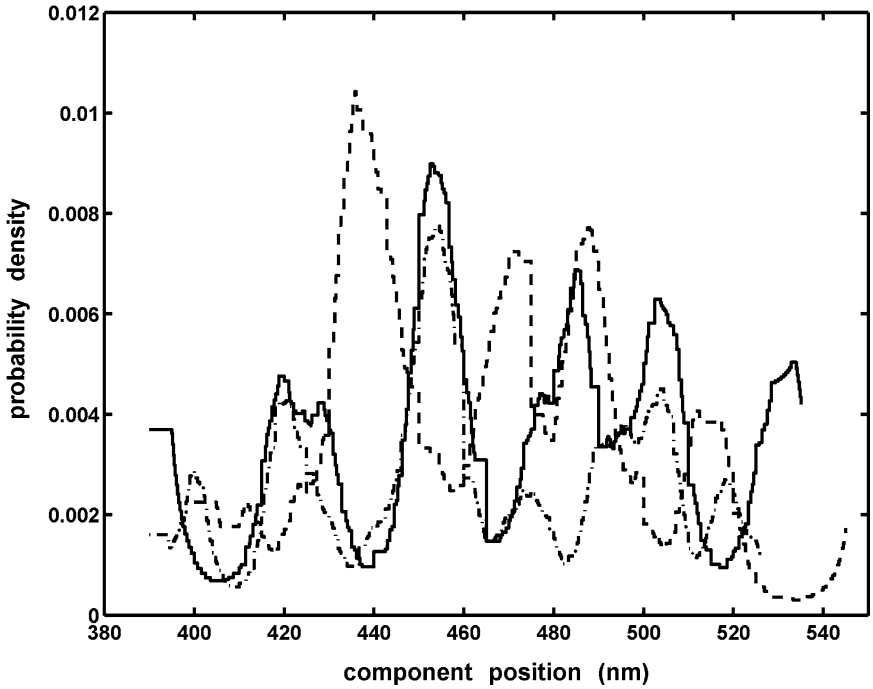

Fig. 7 Approximate distributions of probability densities of component positions for poplar lignin. Emission spectra were deconvoluted with four-component **g4** (- - -), and three-component **ep** (-.-) and **logn** (—) models. The emission spectra were recorded by excitation of lignin at different wavelengths, in the range 360 nm–440 nm, with 5 nm step. Most asymmetric and symmetric components tended to group in alternating positions, similar to the examples presented on lower panels of Figs 5 and 6.

(Fig. 4, upper right, lower right and lower left panels, respectively).

Results of calculation of probability densities of component positions for the mixture of coniferyl alcohol and hydroquinone are presented in Fig. 5. In addition, the corresponding distributions for the two separate molecules (hydroquinone and coniferyl alcohol) are overlaid with them as a reference. By comparing the three panels of Fig. 5, the advantage of asymmetric models over Gaussian becomes obvious. There is a good match in maxima positions of the probability densities between each asymmetric component in the mixture and the corresponding molecular species fitted separately (two upper panels). However, in case of the four-component Gaussian deconvolution, this match is absent (lower panel of Fig. 5).

This procedure was repeated for the second mixture–tryptophan and hydroquinone, these two molecules having more distant emission maxima than coniferyl alcohol and hydroquinone. The results, presented in Fig. 6, are in accordance with those obtained for the first analyzed mixture, favoring the asymmetric models.

In the above analyses we compared two-component asymmetric with four-component Gaussian deconvolution results because, according to the fitting errors presented in Fig. 1, either one asymmetric or at least two Gaussian components are needed to describe an emission band from one fluoropohore. In more complex cases however, such as multicomponent deconvolution of multifluorophore polymers, this numerical relationship may be less strict. Namely, in such systems, if a series of emission spectra with varying excitation wavelength is being analyzed, the number of components used for deconvolution may not necessarily be equal to the number of wavelengths around which the components tend to group. In most cases, the algorithm uses two Gussian components to describe only the most excited fluorophore at that moment. Such an example is presented in Fig. 7, where the probability density distribution of component positions is shown in case of poplar lignin, for the three-component **ep** and **logn,** as well as four-component Gaussian deconvolution. Except for one spectral region, here Gaussian and asymmetric components also tended to group in alternating positions, extending the regularity observed in case of the binary mixtures and five separate molecular species.

Results presented in this work indicate that even in case of simple emission spectra one cannot rely on the positions of symmetric components for tentative fluorophore identification. In complex cases, such as multifluorophore polymers, they may be used only as an indicator of the discrete nature of emission, or eventually assessment of the number of fluorophores, only when corroborated by other experimental approaches [6]. Using correct asymmetric models may mean a step forward in identifying the existing fluorophores in complex molecules, but to which extent–remains to be determined.

Acknowledgements Grant 143043 from the Ministry of Science and Environmental protection of the Republic of Serbia supported this study. We thank Prof Catherine Lapierre, l'Unité de Chimie Biologique INRA-INAPG, Institut National Agronomique Thiverval-Grignon, France, for

providing us with the sample of lignin isolated from poplar (*Populus tremuloides*, clone 1214).

References

1. Andersen CM, Bro R (2003) Practical aspects of PARAFAC modeling of fluorescence excitation-emission data. J Chemometrics 17:200–215
2. Stedmon CA, Markager S, Bro R (2003) Tracing dissolved organic matter in aquatic environments using a new approach to fluorescence spectroscopy. Marine Chem 82:239–254
3. Siano DB, Metzler DE (1969) Band shapes of the electronic spectra of complex molecules. J Chem Phys 51:1856–1861
4. Burstein EA, Emelyanenko VI (1996) Log-normal description of fluorescence spectra of organic fluorophores. Photochem Photobiol 64:316–320
5. Burstein EA, Abornev SM, Reshetnyak YK (2001) Decomposition of protein tryptophan fluorescence spectra into log-normal components. I. Decomposition Algorithms. Biophys J 81:1699–1709
6. Radotić K, Kalauzi A, Djikanović D, Jeremić M, Leblanc R, Cerović Z (2006) Component analysis of the fluorescent spectra of a lignin model compound. J Photochem Photobiol B: Biol 83:1–10